RSC Advances

PAPER

View Article Online
View Journal | View Issue

Cite this: *RSC Adv.*, 2021, **11**, 20746

Homo–hetero/core–shell structure design strategy of $NaYF_4$ nanocrystals for superior upconversion luminescence

Raheel Ahmed Janjua,*[a] Obaid Iqbal,[b] Muhammad Aqeel Ahmed,[c] Abdullah A. Al-Kahtani,*[d] Sara Saeed,[e] Muhammad Imran[f] and Abdul Ghafar Wattoo*[g]

A comprehensive strategy has been developed to construct nano-sized homogeneous and heterogeneous core/shell structures of $NaYF_4$ host. Synthesis conditions of cubic phase/α-$NaYF_4$ and hexagonal phase/β-$NaYF_4$ are discussed. Pure cubic $NaYF_4$:Yb,Er nanocrystals were synthesized with different average sizes extending from 7 nm to 15 nm by varying the reaction time. Temperature and time thresholds of hexagonal nucleation were determined and utilized for controlled core/shell structures of different phases. α-$NaYF_4$:Yb,Er@α-$NaYF_4$, α-$NaYF_4$:Yb,Er@β-$NaYF_4$, β-$NaYF_4$:Yb,Er@α-$NaYF_4$, and β-$NaYF_4$:Yb,Er@β-$NaYF_4$ core/shell structures were prepared by adopting the required conditions to achieve the desired phase. Excess sodium was used to grow hexagonal shell over metastable cubic core under controlled conditions of reaction time and temperature to prevent the structural transition of the core. Upconversion emission spectra have also been obtained. UCL integrated intensities demonstrated about 5-fold enhancement for α-shell over α-core as compared to the core alone and 22-fold enhancement with β-shell. On the other hand, α-shell over β-core exhibited 5-fold enhancement and β-shell over β-core exhibited 6-fold enhancement.

Received 18th March 2021
Accepted 25th May 2021

DOI: 10.1039/d1ra02157e

rsc.li/rsc-advances

Introduction

Up-converting nano-materials has attracted considerable attention due to their broad utility in bio-applications,[1–7] 3D display devices,[8–11] printing,[12–14] lasers[15,16] and storage devices.[17] Up-converters are normally excited by NIR, which allows deep penetration through living cells without damaging them, prevents auto-fluorescence, has a high signal to noise ratio, and is a fast thermal imaging technique.[18–22] UCL studies mainly revolve around Ln-doped halides[23–25] and oxides.[26–28] Among these, Ln-$NaYF_4$ has been the focus of most studies due to its efficient UCL properties.[29,30] However, high efficiency has always been an urgent demand, for which several strategies have been adopted to improve the efficiency, such as co-doping,[31–35] plasmonic effect and surface modification.[36–39] One of the principle of engineering with nanocrystals is tailoring their surfaces.[40–44] Nanocrystalline cores have suffered some issues due to high surface to volume ratio, boundary defects, and ligands.[45–47] These issues tend to quench the luminescence of the core. Surface passivation by inert shell structures has been a proven tool to enhance luminescence.[40,42–44] Therefore, the formation of a shell solves this problem. Core–shell structures are also used for multiple functions such as drug delivery, photodynamic therapy,[18,20,22] and multicolor displays.[24]

Several studies have shown that the growth of a shell around the $NaYF_4$ core enhances the UCL efficiency by improving the transfer of excitation and emission energy to the inner core from the boundaries. A thin shell can passivate the surface of the core by reducing the defects, and control UCL quenching caused by ligands and other impurities.[37,42,43,48–50] $NaYF_4$ exists in cubic and hexagonal phases at ambient conditions. So, different groups proposed different strategies to synthesize core–shell structures with different combinations of phases. Yan *et al.*[51] adopted a two-step growth method to synthesize core–shell $NaYF_4$ with cubic core/cubic shell and hexagonal core/cubic shell. They observed a significant enhancement in the intensity of green emission and further attributed this enhancement to the repair of surface defects and ligands by shell formation. Zhang *et al.*[52] reported hexagonal phase core

[a]*National Engineering Research Center for Optical Instruments, College of Optical Science and Engineering, Zhejiang University, Hangzhou 310058, China. E-mail: raheel@mail.ustc.edu.cn*

[b]*National Synchrotron Radiation Laboratory, Anhui Provincial Engineering Laboratory of Advanced Functional Polymer Film, CAS Key Laboratory of Soft Matter Chemistry, University of Science and Technology of China, Hefei 230026, China*

[c]*Department of Electronics, Quaid-i-Azam University, Islamabad, Pakistan*

[d]*Chemistry Department, College of Science, King Saud University, P.O. Box 2455, Riyadh 11451, Saudi Arabia*

[e]*Department of Physics, University of Science and Technology of China, Hefei, Anhui, China*

[f]*Department of Chemistry, Faculty of Science, King Khalid University, P.O. Box 9004, Abha 61413, Saudi Arabia*

[g]*Department of Physics, Khwaja Fareed University of Engineering and Information Technology, Rahim Yar Khan 64200, Pakistan*

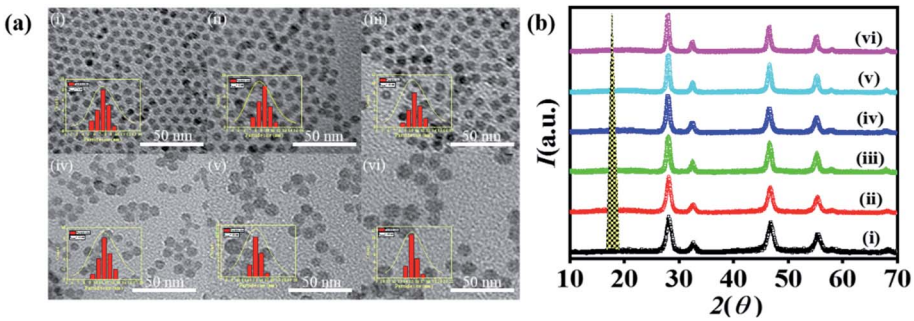

Fig. 1 (a) TEM images with inset size distributions of monodispersed nanocrystals of cubic phase $NaYF_4$:Yb,Er synthesized at $T = 280$ °C for different reaction time (i) 30 min, (ii) 1 h, (iii) 1.5 h, (iv) 2 h, (v) 2.5 h and (vi) 3 h. (b) XRD patterns of $NaYF_4$:Yb,Er synthesized at $T = 300$ °C for different reaction time (i) 30 min, (ii) 60 min, (iii) 90 min, (iv) 120 min, (v) 150 min and (vi) 180 min. (c) Shows the growth of particle size with increasing time of reaction.

and hexagonal phase shell and concluded that the red to green ratio of emission bands was significantly affected by excitation power in the core but remained unchanged in core/shell. van Veggel *et al.*[53] floated a novel strategy to synthesize cubic core and hexagonal shell. Zhao *et al.*[54] also grew hexagonal phase shells induced by the heterogeneous cubic core as a strategy of controlling the small size in the hexagonal phase. Different combinations of core/shell on the basis of structure exhibited their own advantages. Few contributions have been made, but a detailed study is still required that provides better control to synthesize UCL core/shell structures with all possible combinations of phases. In this work, we proposed a comprehensive strategy to design homogeneous and heterogeneous core/shell structures. Every possible combination of core/shell with respect to structural symmetry requires its own synthesis conditions. Homo-structures of $NaYF_4$ is recommended under similar conditions of temperature to avoid secondary phase impurities. $NaYF_4$ with hetero-structure fabrications has more difficulties due to the thermally motivated transition of the cubic phase to the hexagonal phase.[55] If the hexagonal shell is grown over the cubic core at a certain temperature suitable for hexagonal nucleation, then the metastable core also undergoes a phase transition to the hexagonal phase. Our previous approach[56] of sub-10 nm synthesis of hexagonal phase by the use of excess sodium has been used as a key to synthesizing hexagonal shell over cubic core under controlled condition of temperature, which prevents the transformation of the cubic phase core to hexagonal phase. Also, cubic phase core nanocrystals have been synthesized with different sizes to check the stability of the cubic phase for different durations of heating. Therefore, in this effort, we have addressed different synthesis conditions to achieve better control over the fabrication of core–shell structures. $NaYF_4$ in this study may act as a prototype for the synthesis of other similar structures.

Results and discussion

Effect of heating on the size of the cubic phase

Fig. 1a shows TEM images of cubic phase $NaYF_4$:Yb,Er. Nanocrystals are mono-dispersed and spherical in shape with an average size of 7 nm to 15 nm. The size distributions are also shown in the inset of Fig. 1a. The particles were prepared by adopting the reported procedure with slight modification. All the samples were prepared with a fixed composition of precursors in 1-octadecene and oleic acid at a temperature of 280 °C.

Only the heating time has been varied from 30 min to 180 min. When the solution was heated at 280 °C for 30 min, pure cubic phase $NaYF_4$:Yb,Er was obtained, which is confirmed by X-ray diffraction measurement, as shown in Fig. 1b. The nanoparticles exhibited an average size of 7 nm.

When the heating time was increased to 1 hour, the average size of the particles was 9 nm. Similarly, as the heating time was further increased to 1.5 hours, 2 hours, 2.5 hours, and 3 hours, the average size of the obtained particles was 10 nm, 11 nm, 13 nm and 15 nm, respectively. All the reactions yielded a pure cubic phase without the formation of secondary phases. The crystallinity and phase of all the samples were determined by the X-ray diffraction patterns shown in Fig. 1b. Normalized intensities of six samples were plotted against 2θ from 10 to 70. The planes labeled as (111), (200), (220), (311), (222) and (400) corresponded to the cubic symmetry of the JCPDS file no. 77-2042.[57] Crystallite sizes measured using the Debye–Scherrer formula were also consistent with the particle sizes calculated from the TEM images shown in Table 1.

Effect of temperature on the α- to β-phase transition

A series of experiments were performed with increasing temperature to investigate the hexagonal nucleation temperature threshold. When the solution was heated at 300 °C for 30 min, a pure cubic phase was obtained. When the reaction

Table 1 Particle size of cubic phase $NaYF_4$:Yb,Er measured from TEM images and calculated by Scherrer's equation

Reaction time (min)	Particle size calculated from TEM	Crystallite size by calculated Scherrer's equation
30	7	7.060
60	9	8.509
90	10	9.808
120	11	10.790
150	13	12.826
180	15	14.563

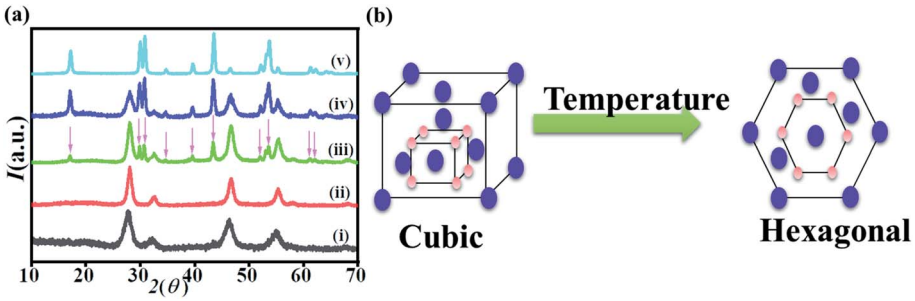

Fig. 2 (a) XRD patterns of $NaYF_4$:Yb,Er synthesized at $T = 300$ °C for different reaction time (i) 30 min, (ii) 60 min, (iii) 90 min, (iv) 120 min and (v) 150 min. (b) Schematic figure shows the phase transition from cubic to hexagonal after prolonged heating.

time was prolonged to 1 hour, 1.5 hours, 2 hours and 2.5 hours with the reaction temperature of 300 °C, the little hexagonal phase peaks appeared at 90 min and became sharper after 120 min of heating. The XRD peaks corresponding to the hexagonal phase according to JCPDS file no. 16-0334 (ref. 57) are marked with an asterisk, as shown in Fig. 2a. After the reaction time of 150 min, pure hexagonal phase was obtained. These observations of reaction time and temperatures were very useful to synthesize homo–hetero core–shell structures.

Synthesis of α-$NaYF_4$:Yb,Er@α-$NaYF_4$

Cubic phase $NaYF_4$:Yb,Er prepared at 280 °C for 60 min was used as the core. The dispersed α-$NaYF_4$:Yb,Er nanocrystals were introduced to the solution at 70 °C until hexane was evaporated completely. Then, the temperature of the reaction was raised to 280 °C and kept for 30 min. α-$NaYF_4$:Yb,Er served as seed, and the shell was formed around α-$NaYF_4$:Yb,Er. TEM images in Fig. 3c show the core/shell $NaYF_4$:Yb,Er@$NaYF_4$. The thickness of the shell was approximately 2 nm. X-ray diffraction patterns in Fig. 3a confirmed that the shell was pure cubic phase.

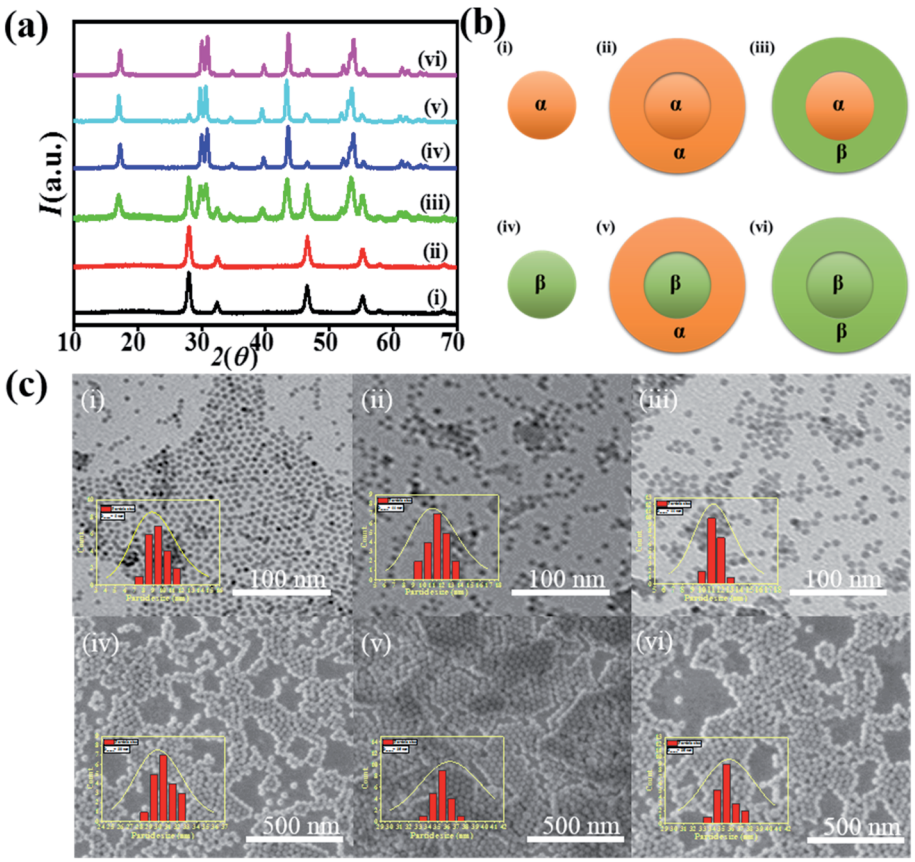

Fig. 3 (a) XRD patterns of core/shell $NaYF_4$ with Yb and Er doped in core. The phase combination consist of (i) α-$NaYF_4$:Yb,Er, (ii) α-$NaYF_4$:Yb,Er@α-$NaYF_4$, (iii) α-$NaYF_4$:Yb,Er@β-$NaYF_4$, (iv) β-$NaYF_4$:Yb,Er, (v) β-$NaYF_4$:Yb,Er@α-$NaYF_4$, and (vi) β-$NaYF_4$:Yb,Er@β-$NaYF_4$. (b) Shows the combinations of the core/shell structure. (c) TEM images of core/shell and the size distributions inset with (i) α-$NaYF_4$:Yb,Er, (ii) α-$NaYF_4$:Yb,Er@α-$NaYF_4$, (iii) α-$NaYF_4$:Yb,Er@β-$NaYF_4$, and FESEM images of (iv) β-$NaYF_4$:Yb,Er, (v) β-$NaYF_4$:Yb,Er@α-$NaYF_4$, and (vi) β-$NaYF_4$:Yb,Er@β-NaYF.

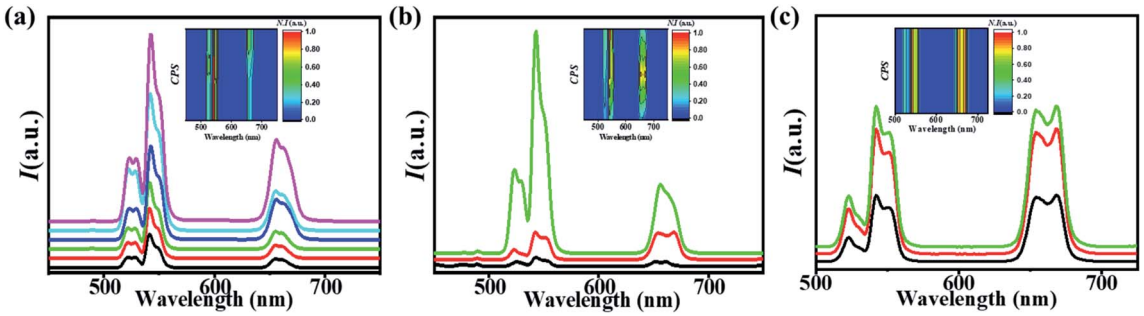

Fig. 4 (a) UC luminescence spectra of α-$NaYF_4$:Yb,Er with sizes from 7 nm to 15 nm. (b) UC luminescence spectra of α-$NaYF_4$:Yb,Er, α-$NaYF_4$:Yb,Er@α-$NaYF_4$, and α-$NaYF_4$:Yb,Er@β-$NaYF_4$. (c) UC luminescence spectra of β-$NaYF_4$:Yb,Er, β-$NaYF_4$:Yb,Er@α-$NaYF_4$, and β-$NaYF_4$:Yb,Er@β-$NaYF_4$.

Synthesis of α-$NaYF_4$:Yb, Er@β-$NaYF_4$

α-$NaYF_4$ nanocrystals prepared at 300 °C for 30 min were used as the core for the β-$NaYF_4$ shell. The β-shell is very critical to synthesize because the nucleation of β-$NaYF_4$ occurs at high temperature for a longer time, and if the reaction proceeds at high temperature for a longer time, then the α-phase core particles that are thermally metastable will naturally transform to β-phase particles by the Ostwald ripening process. Therefore, a different strategy is required here to synthesize the β-shell around the α-core at the minimum possible temperature within a short time period so as to prevent the phase transition of α-seeds. Keeping all situation under consideration, we employed our recent reported strategy of Na^+ driven nucleation of β-$NaYF_4$:Yb,Er. Excess sodium precursor has been used to lower the nucleation threshold for the $NaYF_4$ shell, keeping the α-core stable. Therefore, the solution for the shell was prepared with excess sodium instead of a stoichiometric amount. The solution was heated for 30 min at 300 °C to grow a shell around the α-core. Since the temperature was low enough for a shorter time, it will not affect the phase of the α-core. X-ray diffraction of the α-core/β-shell is shown in Fig. 3a. The patterns show the peaks of the α-phase and β-phase. TEM images in Fig. 3c show uniform morphology of the core–shell structure with the size distributions in the inset.

Synthesis of β-$NaYF_4$:Yb,Er@α-$NaYF_4$

α-Shell over β-core was grown by using the general precursors. The reaction temperature was 300 °C for 30 min. FESEM image in Fig. 3b(v) shows the β-core–α-shell morphology with an average size of 35 nm. Uniform clear core/shell structures are formed. X-ray diffraction analysis confirms the formation of α-shell over pure β-core.

Synthesis of β-$NaYF_4$:Yb,Er@β-$NaYF_4$

β-Shell was grown over β-shell by heating the standard concentration of the precursor solution at 300 °C for 1.5 hours in the presence of the β-core. The core–shell morphology is shown in Fig. 3c(vi). The estimated core/shell thickness was 35 nm. X-ray diffraction patterns confirm that pure β-shell has been grown.

Upconversion luminescence

Fig. 4a shows the up-conversion emission spectra of the cubic phase $NaYF_4$:Yb,Er nanocrystals of varying sizes. All nanocrystals exhibited up-conversion emission in green and red when excited with 980 nm NIR radiation. Green emissions were observed at about 540 nm, which can be ascribed to the $^2H_{11/2}$, $^4S_{3/2} \rightarrow {}^4I_{15/2}$ transitions. Red emission band centered at 660 nm has been obtained due to the $^4F_{7/2} \rightarrow {}^4I_{15/2}$ transitions. It is apparent that the luminescence of cubic nanocrystals increases with increasing particle size, which is consistent with the previous study.

Fig. 4b and c demonstrate the up-conversion emission enhancement in the core/shell structure of $NaYF_4$:Yb,Er as compared to the core alone. The β-shell exhibits more intense luminescence as compared to the α-shell. The β-shell serves as a better shield of defects as compared to the α-shell. The plausible reason for better enhancement in the case of the β-shell is a high density of β-phase $NaYF_4$. The high-density layer provided a better cure to surface defects. Core/shell structures also have shown the enhancement of up-conversion luminescence with the β-core.

α-Shell over β-core proves to be a good protector of defects and other impurities by enhancing the luminescence. The β-shell comes out superior to the α-shell as it enhances the luminescence more than the α-coating. The enhancement factor for core–shell structures has been calculated from the integrated intensities of emission. α-Core/α-shell yielded about 5-fold enhancement as compared to the α-core, whereas α-core/β-shell exhibited 22-fold enhancement. In the case of the β-core, α-shell with β-core produced 5-fold enhancement and β-shell over β-core produced 6-fold enhancement. All the UCL for core/shell structures as compared to the core alone are summarized in Table 2.

Table 2 Φ and Ψ show the arbitrary UCL of cubic and hexagonal cores, respectively, and the enhancement factors as their multiples are measured for shell structures

Structure of particle	UCL enhancement factor
α-$NaYF_4$:Yb,Er	1Φ
α-$NaYF_4$:Yb,Er@α-$NaYF_4$	5Φ
α-$NaYF_4$:Yb,Er@β-$NaYF_4$	22Φ
β-$NaYF_4$:Yb,Er	1Ψ
β-$NaYF_4$:Yb,Er@α-$NaYF_4$	5Ψ
β-$NaYF_4$:Yb,Er@β-$NaYF_4$	6Ψ

Conclusion

$NaYF_4$ has been used as a prototype to propose a detailed strategy for synthesizing core/shell structures at nanoscale. The synthesis conditions of two structures of $NaYF_4$, which are cubic and hexagonal, were discussed in detail. Each crystal symmetry had its own synthesis conditions, which were determined in this work. Size-dependent cubic phase nanocrystals were synthesized by varying the reaction time. A longer heating time yielded larger particles. The UCL intensities were also stronger for larger particles. Core/shell structures with the following combinations were prepared: α-$NaYF_4$:Yb,Er@α-$NaYF_4$, α-$NaYF_4$:Yb,Er@β-$NaYF_4$, β-$NaYF_4$:Yb,Er@α-$NaYF_4$, and β-$NaYF_4$:Yb,Er@β-$NaYF_4$. The cubic shell was grown over the cubic core and hexagonal core by using suitable conditions. Hexagonal shell over cubic core was grown using excess sodium to lower the nucleation threshold of hexagonal symmetry. This helped to prevent the conversion of the metastable cubic core to the hexagonal phase. Upconversion luminescence spectra of all prepared samples were determined. Enhancement was observed after shell formation.

Methods

Synthesis section

Reagents. Rare-earth chlorides were bought from Aladdin, whereas, SCR Chemicals (Pty) Ltd. was the source of sodium acetate, sodium hydroxide and ammonium fluoride. RE-oleates were prepared by adopting the procedure after considerable modification specified in the literature.[58]

Synthesis of hexagonal phase $NaYF_4$:Yb,Er

For the synthesis of sub-10 nm of hexagonal phase $NaYF_4$:Er,Yb, 1 mmol of RE-oleates (0.8 : 0.18 : 0.02/Y : Yb : Er ratio) and 7 mmol of sodium acetate were dissolved in 10 mL ethanol in a three-necked glass flask. 5 mL of 1-octadecene mixed with 10 mL of oleic acid was then added to the above solution, which was heated at 60 °C until all the ethanol was evaporated. The solution was further heated to an elevated temperature of 160 °C for 30 min under the steady flow of Ar gas. The solution was then cooled down to room temperature when the residual gases were removed. Next, 4 mmol of NH_4F and 2.5 mmol of NaOH were mixed in 10 mL of methanol and then transferred to the three-necked flask. The flask containing the mixture was heated to 300 °C with a revolution rate of 20 °C per min for 30 min. It was then left to cool naturally to ambient temperature and the product precipitated in acetone. The precipitate was centrifuged to get the sample and then washed several times with ethanol. The samples were collected after centrifugation and dispersed in hexane.

Synthesis of cubic phase $NaYF_4$:Yb,Er

A similar synthesis procedure was adopted for the sub-10 nm cubic phase $NaYF_4$:Er,Yb by varying concentrations of the reactants and reaction time. 1 mmol of rare-earth oleates (0.8 : 0.18 : 0.02/Y : Yb : Er ratio) were dissolved in 10 mL of ethane. 5 mL of 1-octadecene and 10 mL of oleic acid were used. 4 mmol of NH_4F and 2.5 mmol of NaOH were mixed in 10 mL of methanol. The mixture was heated to 280 °C at the rate of 20 °C per min for 30 min. The samples were collected after centrifugation and dispersed in hexane. When the reaction time was varied from 30 min to 60 min, the particle sizes changed from 7 nm to 9 nm. Similarly, as the heating time was raised to 1.5 hours, 2 hours, 2.5 hours, and 3 hours, the average size of the obtained particles became 10 nm, 11 nm, 13 nm and 15 nm, respectively.

Sample characterization

Morphological measurements were performed with High-Resolution Transmission Electron Microscopy (JEOL-2010) to measure the particle size and identify the shape. The phase and structure identification were achieved by X-ray diffraction studies (Rigaku SmartLab diffractometer) by employing Cu-Kα radiation ($\lambda = 0.154056$ nm). Emission spectra were obtained on a fluorescence spectrometer (Princeton Instruments Acton SP 2750) equipped with an excitation source of 980 nm laser. Pellets of each nanocrystal were prepared to measure the spectra.

Funding

The authors extend their appreciation to the Deanship of Scientific Research at King Saud University for funding this work through Research Group No. RG-1441-5070. M. Imran expresses appreciation to the Deanship of Scientific Research at King Khalid University Saudi Arabia for funding through research group program under grant number R.G.P. 2/28/42.

Conflicts of interest

There are no conflicts to declare.

References

1 M. D. Slater, D. Kim, E. Lee and C. S. Johnson, *Adv. Funct. Mater.*, 2013, **23**, 947–958.
2 D. Kundu, E. Talaie, V. Duffort and L. F. Nazar, *Angew. Chem., Int. Ed.*, 2015, **54**, 3432–3448.
3 D. Larcher and J. M. Tarascon, *Nat. Chem.*, 2015, **7**, 19–29.
4 J. Liang, F. Li and H. M. Cheng, *Energy Storage Materials*, 2017, **7**, A1–A3.
5 B. Scrosati, *J. Solid State Electrochem.*, 2011, **15**, 1623–1630.
6 C. Vaalma, D. Buchholz, M. Weil and S. Passerini, *Nat. Rev. Mater.*, 2018, 18013.
7 L. Wang, Q. Wang, W. Jia, S. Chen, P. Gao and J. Li, *J. Power Sources*, 2017, **342**, 175–182.
8 Y. Cheng, J. Huang, J. Li, Z. Xu, L. Cao, H. Ouyang, J. Yan and H. Qi, *J. Alloys Compd.*, 2016, **658**, 234–240.
9 B. Qu, C. Ma, G. Ji, C. Xu, J. Xu, Y. S. Meng, T. Wang and J. Y. Lee, *Adv. Mater.*, 2014, **26**, 3854–3859.
10 X. Xie, Z. Ao, D. Su, J. Zhang and G. Wang, *Adv. Funct. Mater.*, 2015, **25**, 1393–1403.

11 Z. Hu, L. Wang, K. Zhang, J. Wang, F. Cheng, Z. Tao and J. Chen, *Angew. Chem., Int. Ed.*, 2014, **53**, 12794–12798.
12 M. Wilkening and P. Heitjans, *Phys. Rev. B: Condens. Matter Mater. Phys.*, 2008, **77**, 1–13.
13 M. Wilkening, W. Küchler and P. Heitjans, *Phys. Rev. Lett.*, 2006, **97**, 1–4.
14 A. van Der Ven, J. Bhattacharya and A. A. Belak, *Acc. Chem. Res.*, 2013, **46**, 1216–1225.
15 G. H. Newman and L. P. Klemann, *J. Electrochem. Soc.*, 1980, 2097.
16 D. A. Winn, J. M. Shemilt and B. C. H. Steele, *Mater. Res. Bull.*, 1976, **11**, 559–566.
17 Y. Liu, H. Wang, L. Cheng and N. Han, *Nano Energy*, 2016, **20**, 168–175.
18 Z. Hou, C. Li, P. Ma, Z. Cheng, X. Li, X. Zhang, Y. Dai, D. Yang, H. Lian and J. Lin, *Adv. Funct. Mater.*, 2012, **22**, 2713–2722.
19 L. Liang, Y. Liu and X. Z. Zhao, *Chem. Commun.*, 2013, **49**, 3958.
20 X. Liu, M. Zheng, X. Kong, Y. Zhang, Q. Zeng, Z. Sun, W. J. Buma and H. Zhang, *Chem. Commun.*, 2013, **49**, 3224–3226.
21 A. Podhorodecki, M. Banski, A. Noculak, B. Sojka, G. Pawlik and J. Misiewicz, *Nanoscale*, 2013, **5**, 429–436.
22 Q. Xiao, Y. Ji, Z. Xiao, Y. Zhang, H. Lin and Q. Wang, *Chem. Commun.*, 2013, **49**, 1527–1529.
23 J. C. Boyer, F. Vetrone, L. A. Cuccia and J. A. Capobianco, *J. Am. Chem. Soc.*, 2006, **128**, 7444–7445.
24 S. Heer, K. Kömpe, H. U. Güdel and M. Haase, *Adv. Mater.*, 2004, **16**, 2102–2105.
25 H. U. Gu, M. Pollnau, D. R. Gamelin and S. R. Lu, *Phys. Rev. B: Condens. Matter Mater. Phys.*, 2000, **61**, 3337.
26 A. Patra, C. S. Friend, R. Kapoor and P. N. Prasad, *Chem. Mater.*, 2003, **15**, 3650–3655.
27 A. Patra, C. S. Friend, R. Kapoor and P. N. Prasad, *J. Phys. Chem. B*, 2002, **106**, 1909–1912.
28 Q. Lu, Y. Hou, A. Tang, H. Wu and F. Teng, *Appl. Phys. Lett.*, 2013, **102**(23), 233103.
29 D. Kumar, K. Verma, S. Verma, B. Chaudhary, S. Som, V. Sharma, V. Kumar and H. C. Swart, *Phys. B*, 2018, **535**, 278–286.
30 R. A. Janjua, U. Farooq, R. Dai, Z. Wang and Z. Zhang, *Opt. Lett.*, 2019, **44**, 4678.
31 Y. Wang, R. Cai and Z. Liu, *CrystEngComm*, 2011, **13**, 1772–1774.
32 F. Wang and X. Liu, *Chem. Soc. Rev.*, 2009, **38**, 976–989.
33 P. Qiu, N. Zhou, H. Chen, C. Zhang, G. Gao and D. Cui, *Nanoscale*, 2013, **5**, 11512–11525.
34 H. Na, K. Woo, K. Lim and H. S. Jang, *Nanoscale*, 2013, **5**, 4242–4251.
35 Q. Dou and Y. Zhang, *Langmuir*, 2011, **27**, 13236–13241.
36 Y. Ma, H. Liu, Z. Han, L. Yang, B. Sun and J. Liu, *Analyst*, 2014, **139**, 5983–5988.
37 S. Schietinger, T. Aichele, H. Q. Wang, T. Nann and O. Benson, *Nano Lett.*, 2010, **10**, 134–138.
38 D. M. Wu, A. García-Etxarri, A. Salleo and J. A. Dionne, *J. Phys. Chem. Lett.*, 2014, **5**, 4020–4031.
39 H. Zhang, Y. Li, I. A. Ivanov, Y. Qu, Y. Huang and X. Duan, *Angew. Chem., Int. Ed.*, 2010, **49**, 2865–2868.
40 H. Guo, Z. Li, H. Qian, Y. Hu and I. N. Muhammad, *Nanotechnology*, 2010, **21**(12), 125602.
41 J. Pichaandi, F. C. J. M. van Veggel and M. Raudsepp, *ACS Appl. Mater. Interfaces*, 2010, **2**, 157–164.
42 F. Vetrone, R. Naccache, V. Mahalingam, C. G. Morgan and J. A. Capobianco, *Adv. Funct. Mater.*, 2009, **19**, 2924–2929.
43 G. S. Yi and G. M. Chow, *Chem. Mater.*, 2007, **19**, 341–343.
44 J. Zhao, Y. Sun, X. Kong, L. Tian, Y. Wang, L. Tu, J. Zhao and H. Zhang, *J. Phys. Chem. B*, 2008, **112**, 15666–15672.
45 K. W. Krämer, D. Biner, G. Frei, H. U. Güdel, M. P. Hehlen and S. R. Lüthi, *Chem. Mater.*, 2004, **16**, 1244–1251.
46 J. Shan, M. Uddi, R. Wei, N. Yao and Y. Ju, *J. Phys. Chem. C*, 2010, **114**, 2452–2461.
47 L. Wang and Y. Li, *Nano Lett.*, 2006, **6**, 1645–1649.
48 C. Homann, L. Krukewitt, F. Frenzel, B. Grauel, C. Würth, U. Resch-Genger and M. Haase, *Angew. Chem.*, 2018, **130**, 8901–8905.
49 H. Guo, Z. Li, H. Qian, Y. Hu and I. N. Muhammad, *Nanotechnology*, 2008, **24**, 12123–12125.
50 Y. Wang, L. Tu, J. Zhao, Y. Sun, X. Kong and H. Zhang, *J. Phys. Chem. C*, 2009, **113**, 7164–7169.
51 H. Mai, Y. Zhang, L. Sun and C. Yan, *J. Phys. Chem. C*, 2007, 13721–13729.
52 Y. Wang, L. Tu, J. Zhao, Y. Sun, X. Kong and H. Zhang, *J. Phys. Chem. C*, 2009, 7164–7169.
53 N. J. J. Johnson, A. Korinek, C. Dong and F. C. J. M. van Veggel, *J. Am. Chem. Soc.*, 2012, **134**(27), 11068–11071.
54 D. Zhao, H. Chen, P. Zhang, H. Cui and W. Qin, *Nanoscale Res. Lett.*, 2017, **12**(1), DOI: 10.1186/s11671-017-2306-3.
55 H. Mai, Y. Zhang, L. Sun and C. Yan, *J. Phys. Chem. C*, 2007, 13730–13739.
56 R. A. Janjua, C. Gao, R. Dai, Z. Sui, M. A. Ahmad Raja, Z. Wang, X. Zhen and Z. Zhang, *J. Phys. Chem. C*, 2018, **122**, 23242–23250.
57 L. Wang, X. Li, Z. Li, W. Chu, R. Li, K. Lin, H. Qian, Y. Wang, C. Wu, J. Li, D. Tu, Q. Zhang, L. Song, J. Jiang, X. Chen, Y. Luo, Y. Xie and Y. Xiong, *Adv. Mater.*, 2015, **27**, 5528–5533.
58 J. Park, K. An, Y. Hwang, J.-G. Park, H. J. Noh, J. Y. Kim, J. H. Park, N. M. Hwang and T. Hyeon, *Nat. Mater.*, 2004, **3**, 891–895.